

Cycles, randomness, and transport from chaotic dynamics to stochastic processes

Pierre Gaspard

*Center for Nonlinear Phenomena and Complex Systems,
Université Libre de Bruxelles, Code Postal 231, Campus Plaine, B-1050 Brussels, Belgium*

An overview is given of advances at the frontier between dynamical systems theory and nonequilibrium statistical mechanics. Sensitivity to initial conditions is a mechanism at the origin of dynamical randomness – alias temporal disorder – in deterministic dynamical systems. In spatially extended systems sustaining transport processes such as diffusion, relationships can be established between the characteristic quantities of dynamical chaos and the transport coefficients, bringing new insight into the second law of thermodynamics. With methods from dynamical systems theory, the microscopic time-reversal symmetry can be shown to be broken at the statistical level of description in nonequilibrium systems. In this way, the thermodynamic entropy production turns out to be related to temporal disorder and its time asymmetry away from equilibrium.

I. INTRODUCTION

Random time evolution is observed in many natural phenomena. Sensitivity to initial conditions is a dynamical mechanism allowing us to understand how randomness can be compatible with a deterministic description in terms of ordinary or partial differential equations in time. Although the solution of these differential equations is unique given the initial and boundary conditions, these latter are not fixed by the equations themselves, which is a fundamental source for randomness. This basic feature motivates the introduction of the probabilistic description common to dynamical systems theory and statistical mechanics, opening fruitful perspectives in our understanding of rate and transport processes, decay of correlations, relaxation towards statistical stationarity, and the second law of thermodynamics on fundamental grounds.

The time evolution of natural systems is a major preoccupation of modern science. Newtonian mechanics has provided the basis of a methodology to approach this issue in terms of ordinary differential equations giving the time derivatives of the variables of interest. If this approach historically concerned the motion of celestial bodies in the solar system, many other systems can also be described in similar terms: ordinary differential equations for systems with finite or countable degrees of freedom or partial differential equations for fields evolving in continuous media. During the XIXth century, Cauchy, Kovalevskaya, and others proved the existence and unicity of their solution starting from given initial conditions (and also given boundary conditions for partial differential equations) if the equations of motion are regular enough [1–4]. These proofs constitute the basis of determinism, according to which time evolution is uniquely determined in these schemes by the initial (and boundary) conditions.

However, many phenomena manifest random behavior that are unpredictable. Dice games known for 5000 years or more illustrate such behavior, which has motivated the development of probability theory. In such phenomena, the outcome does not appear to be determined by the known initial conditions. Already Maxwell and Poincaré pointed out the fact that little causes may induce large effects [5, 6]. Therefore, if the cause is so small to remain unnoticed, the effect will appear random, i.e., without apparent cause. Nowadays, this dynamical behavior is known as sensitivity to initial conditions. The importance of this mechanism to generate random processes in deterministic dynamical systems has been demonstrated in particular by the pioneering work of Lorenz in meteorology [7]. Since then, methods have been developed to characterize the sensitivity to initial conditions and the resulting dynamical randomness in dynamical systems theory [8]. Many deterministic systems have been found to be chaotic not only in hydrodynamics [9, 10], but also in molecular dynamics [11–14], chemical and biochemical kinetics including heterogeneous catalysis and electrochemistry [15–17], nonlinear optics [18, 19], population dynamics [20], celestial mechanics [21, 22], astrophysics [23], and beyond.

If the mechanism of sensitivity to initial conditions is specific to nonlinear dynamical systems, a feature common to every deterministic systems is that their initial conditions are not determined by the system itself and they are thus free to take arbitrary values in the continuum of physical states. The larger the state space, the broader the arbitrariness on the initial conditions. In this regard, the equations of motion are incomplete and should be supplemented by assumptions on their initial conditions. In general, the initial conditions are only known with a finite resolution and should thus be assumed to obey some probability distribution. Now, this distribution evolves in time according to the deterministic dynamical system, as carried out by Liouville's equation of nonequilibrium

statistical mechanics [24]. Such a probabilistic scheme applies to systems with a few degrees of freedom, as well as to high-dimensional systems [25]. This statistical approach has led to cross-fertilization between dynamical systems theory and statistical mechanics and a *Chaos* focus issue was devoted in particular to this topic [26]. The aim of the present paper is to highlight several key issues at this frontier.

First, deterministic dynamical systems are the stage of rate processes usually described by kinetic theory. It turns out that, in chaotic systems, the rates are closely related to the quantities characterizing sensitivity to initial conditions and dynamical randomness, which opens broad perspectives to understand irreversible phenomena and transport processes on the basis of the chaotic properties [11–14]. Thanks to these considerations, large-deviation dynamical relationships have been established between the characteristic quantities of chaos, the transport coefficients, as well as other irreversible properties [27–39].

Secondly, the decay and relaxation rates can be obtained by decomposing the dynamics in terms of unstable periodic orbits if they are dense in the chaotic attractor or chaotic saddle of the system [40, 41]. This method can be applied to dynamical systems in the presence or absence of noise [42–44], as well as to quantum systems in the semiclassical limit [45], which provides deep insight into the dynamics of many dissipative and Hamiltonian systems.

Furthermore, dynamical randomness can be conceived as temporal disorder in the time evolution of the system of interest. Deterministic dynamical systems or stochastic processes may display different degrees of randomness, which can be compared quantitatively [46]. In this regard, methods from dynamical systems theory can be extended to the study of stochastic processes, leading to novel approaches to understand the implications of the second law of thermodynamics [47–63].

The paper is organized as follows. Section II explains that a given system may have different levels of description. Each level has specific dynamical properties manifesting themselves on specific time scales. Section III is devoted to the characterization of dynamical randomness from chaotic dynamical systems to stochastic processes. Section IV shows how chaotic dynamics can be decomposed into cycles in periodic-orbit theory, which can be applied as well to noisy and quantum systems. Section V summarizes the relationships between chaotic and transport properties. Conclusions and perspectives are presented in Section VI.

II. GENERALITIES

A. Levels of description

An important aspect of modern science is that the dynamics of one and the same system may be studied at different levels of description from the microscopic to macroscopic scales. Let us consider a large isolated system with N particles of masses $\{m_j\}_{j=1}^N$ interacting with each other. These particles may be N_e electrons and N_n nuclei.

- *The microscopic quantum level of description.* At this level, the system is described by a wavefunction $\Psi(\mathbf{r}_1, \mathbf{r}_2, \dots, \mathbf{r}_N, t)$ defined in the configuration space of the positions $\{\mathbf{r}_j\}_{j=1}^N$ of the particles. The wavefunction belongs to an infinite-dimensional Hilbert space of square-integrable complex functions such that $\int_{\mathbb{R}^{3N}} |\Psi|^2 d^{3N}r = 1$. The time evolution of the wavefunction is ruled by Schrödinger's equation

$$i \hbar \partial_t \Psi = \hat{H} \Psi, \quad (1)$$

where \hbar is Planck's constant and \hat{H} is the Hamiltonian operator:

$$\hat{H} = \sum_{j=1}^N -\frac{\hbar^2}{2m_j} \nabla_j^2 + U(\mathbf{r}_1, \mathbf{r}_2, \dots, \mathbf{r}_N), \quad (2)$$

with the potential energy U [64]. The solution Ψ_t starting from the initial wavefunction Ψ_0 is unique so that this unitary time evolution is deterministic. However, this determinism takes place in the Hilbert space where the preparation of initial conditions is non trivial. Moreover, Schrödinger's equation is linear, which provides coherence to the quantum time evolution. If the energy spectrum is discrete, the time evolution is almost periodic with possible recurrences arbitrarily close to the initial state after long enough time. Such recurrences are absent if the energy spectrum is continuous as in scattering systems or infinitely large quantum systems.

- *The microscopic classical level of description.* Since nuclei are much heavier than electrons, their de Broglie wavelength is smaller than the distance between them at room temperature and atmospheric pressure, which justifies the use of classical mechanics for their description. Under such circumstances, the microscopic dynamics

is ruled by Hamilton's equations

$$\begin{cases} \frac{d\mathbf{r}_j}{dt} = +\frac{\partial H}{\partial \mathbf{p}_j}, \\ \frac{d\mathbf{p}_j}{dt} = -\frac{\partial H}{\partial \mathbf{r}_j}, \end{cases} \quad (3)$$

in terms of the positions and momenta $\{\mathbf{r}_j, \mathbf{p}_j\}_{j=1}^{N_n}$ of nuclei and the Hamiltonian function

$$H = \sum_{j=1}^{N_n} \frac{\mathbf{p}_j^2}{2m_j} + U_n(\mathbf{r}_1, \mathbf{r}_2, \dots, \mathbf{r}_{N_n}), \quad (4)$$

where U_n is the effective Born-Oppenheimer potential energy between the nuclei [64]. This classical dynamics is an approximation of the quantum dynamics in the limit where Planck's constant is small with respect to the actions of the paths followed by the system. In general, Hamilton's equations are nonlinear so that the classical dynamics may present sensitivity to initial conditions with exponential separation between nearby trajectories in the phase space constituted by each energy shell $H = E$, since energy is conserved for autonomous systems.

- *The mesoscopic level of description.* In systems composed of many nuclei, the description is often reduced by coarse graining the microscopic dynamics into a few slowly evolving observables, $x_j = A_j(\mathbf{r}_1, \mathbf{p}_1, \mathbf{r}_2, \mathbf{p}_2, \dots, \mathbf{r}_{N_n}, \mathbf{p}_{N_n})$, such as the position coordinates of a micrometric colloidal particle, the concentrations of molecules of different species, or the local temperature. These slow degrees of freedom are limited in number, $\mathbf{x} = (x_1, x_2, \dots, x_d)$ with $d \ll N_n$. For particular systems, they can be shown to obey stochastic ordinary (or partial) differential equations:

$$\frac{d\mathbf{x}}{dt} = \mathbf{F}(\mathbf{x}) + \sum_{\alpha=1}^{\nu} C_{\alpha}(\mathbf{x}) \xi_{\alpha}(t), \quad (5)$$

where $C_{\alpha}(\mathbf{x})$ are the noise amplitudes [43]. As in Brownian motion, the fluctuations can be described in terms of uncorrelated Gaussian white noises such that $\langle \xi_{\alpha}(t) \rangle = 0$ and $\langle \xi_{\alpha}(t) \xi_{\beta}(t') \rangle = \delta_{\alpha\beta} \delta(t - t')$.

- *The macroscopic level of description.* Scaling up the coarse graining, e.g., by lumping together and renormalizing the observables \mathbf{x} , the noise amplitudes become smaller and smaller in Eq. (5). For instance, Langevin's fluctuating force acting on a micrometric particle suspended in a viscous fluid becomes negligible as the particle diameter increases to millimetric or centimetric sizes. Similarly, the macroscopic equations of fluid mechanics are recovered from the stochastic partial differential equations of fluctuating hydrodynamics [65]. The noiseless limit $C_{\alpha}(\mathbf{x}) \rightarrow 0$ is thus reached at the macroscale and the stochastic differential equations (5) becomes the ordinary differential equations

$$\frac{d\mathbf{x}}{dt} = \mathbf{F}(\mathbf{x}) \quad \text{with} \quad \mathbf{x} \in \mathcal{M} \subseteq \mathbb{R}^d. \quad (6)$$

If the vector field $\mathbf{F}(\mathbf{x})$ obeys Lipschitz' conditions, Cauchy's theorem guarantees the existence and unicity of the solution starting from given initial conditions \mathbf{x}_0 , which defines a flow in the phase space \mathcal{M} : $\mathbf{x}_t = \Phi^t \mathbf{x}_0$ [1, 2]. For partial differential equations, it is the Cauchy-Kovalevskaya theorem that guarantees existence and unicity for given initial and boundary conditions [3, 4].

Each level of description has its own specificities, but the physical properties can be studied at the different levels of description, which allows interesting comparisons. In particular, the time scale of relaxation towards a statistically stationary state assimilated to the state of thermodynamic equilibrium is expected to be obtained in all the levels of description. This allows us to obtain the values of the transport coefficients used at the mesoscopic and macroscopic levels of description from the microscopic dynamics thanks to the Green-Kubo formulas [24, 32]. The same holds for decay rates of various kinds in reactive systems. Recent advances show that the comparison goes beyond these properties and provides novel methods to characterize the dynamical properties of different systems, as explained here below.

B. Probabilistic description

In the description based on Eq. (6), the physical state of the system is defined as a point $\mathbf{x} = (x_1, x_2, \dots, x_d)$ in a d -dimensional phase space $\mathcal{M} \subseteq \mathbb{R}^d$. This phase space forms a continuum because the coordinates x_i are real numbers requiring infinitely many digits for their complete knowledge. However, any experimental measure can only provide a finite number of digits since resolution is always limited. Therefore, even if the system may be assumed to be in a given state \mathbf{x} at time t , the full knowledge of this state is beyond finite resources. Accordingly, the current state \mathbf{x}_t of the system and, in particular, its initial state \mathbf{x}_0 can only be described in terms of probability distributions. The local conservation of probability in phase space implies that any probability density $p(\mathbf{x})$ obeys the generalized Liouvillian equation [25, 31]:

$$\partial_t p = \hat{L} p \equiv -\text{div}(\mathbf{F}p). \quad (7)$$

If the flow Φ^t is invertible, the solution of this Liouvillian equation can be written as

$$p_t(\mathbf{x}) = \left| \det \frac{\partial \Phi^t}{\partial \mathbf{x}}(\Phi^{-t}\mathbf{x}) \right|^{-1} \times p_0(\Phi^{-t}\mathbf{x}) \quad (8)$$

in terms of the initial probability density $p_0(\mathbf{x})$ and

$$\left| \det \frac{\partial \Phi^t}{\partial \mathbf{x}} \right| = \exp \int_0^t \text{div} \mathbf{F} d\tau. \quad (9)$$

The dynamics preserves the phase-space volumes if $\text{div} \mathbf{F} = 0$ so that $\left| \det \frac{\partial \Phi^t}{\partial \mathbf{x}} \right| = 1$, which is the case in Hamiltonian systems. In dissipative systems, the phase-space volumes typically contract because $\left| \det \frac{\partial \Phi^t}{\partial \mathbf{x}} \right| < 1$ for large enough time t .

C. Lyapunov exponents

The sensitivity to initial conditions is characterized by carrying out the linear stability analysis of individual trajectories. The infinitesimal perturbations $\delta \mathbf{x}_t$ of a trajectory \mathbf{x}_t obey equations obtained by linearizing Eq. (6). Lyapunov exponents are defined by considering the growth rates of multidimensional volumes supported by several such linearly independent perturbations:

$$\left| \text{Vol}_i \left(\delta \mathbf{x}_t^{(1)}, \delta \mathbf{x}_t^{(2)}, \dots, \delta \mathbf{x}_t^{(i)} \right) \right| \sim e^{(\lambda_1 + \lambda_2 + \dots + \lambda_i)t} \quad (10)$$

with $i = 1, 2, \dots, d = \dim \mathcal{M}$ [8]. The Lyapunov exponents form a spectrum from the largest down to the smallest: $\lambda_1 \geq \lambda_2 \geq \dots \geq \lambda_d$. The sum of all the Lyapunov exponents is equal to zero in volume-preserving systems, but is negative in dissipative systems.

The system presents sensitivity to initial conditions if some Lyapunov exponents are positive. If positive, the largest Lyapunov exponent λ_1 defines the so-called Lyapunov horizon, beyond which prediction is no longer possible. Indeed, if the initial conditions are known with a resolution $\|\delta \mathbf{x}_0\| = \epsilon_0$, reliable predictions such that $\|\delta \mathbf{x}_t\| < \epsilon$ only last over the finite time interval

$$0 < t < \frac{1}{\lambda_1} \ln \frac{\epsilon}{\epsilon_0}, \quad (11)$$

with $\epsilon > \epsilon_0$. The price to double this interval is to improve the resolution on the initial conditions from ϵ_0 down to ϵ_0^2/ϵ , which is very expensive in practice. In order to manage predictability, it is thus important to determine the values of the Lyapunov exponents.

Methods have been developed for this purpose, not only to compute numerically these exponents, but also to measure them using experimental data. Lyapunov exponents have been measured, in particular, at the onset of hydrodynamic turbulence and in chemical chaos [10, 15, 16, 66]. In high-dimensional systems, important efforts have been devoted to the computation of Lyapunov spectra in turbulence [67], as well as in molecular dynamics for hard-sphere gases and spin systems [11–14, 68–76]. In exceptional limits, analytical expressions can even be obtained for the full Lyapunov spectrum [37, 38].

Furthermore, covariant Lyapunov vectors associated with the exponents have been introduced in order to determine the intrinsic local directions in the phase space of chaotic systems and, thus, the phase-space regions generating sensitivity to initial conditions [77–80]. The Lyapunov modes associated with the exponents vanishing because of fundamental conservation laws have also been investigated [81–84].

D. Ergodic theory

Beyond Lyapunov's horizon of predictability (11), the probabilistic description in terms of the generalized Liouvillian equation (7) becomes essential [25, 93]. In this respect, the methods of ergodic theory are playing an important role to classify the properties expected for the solutions of Eq. (7).

In ergodic theory, a dynamical system $(\mathcal{M}, \Phi^t, p_{\text{st}})$ is defined by its phase space \mathcal{M} , its flow Φ^t , and any normalized stationary probability distribution with a density satisfying $\partial_t p_{\text{st}} = \hat{L} p_{\text{st}} = 0$ [85, 86].

The phase space may be bounded or unbounded [87, 88]. Even if the phase space is unbounded, trajectories can be attracted to bounded phase-space regions in dissipative systems. Hamiltonian systems with an unbounded phase space are of scattering type or sustain transport processes such as diffusion in the periodic Lorentz gases or heating in periodically driven systems, which shows the large variety of possible dynamical systems [31].

If the phase space is bounded or if the trajectories move towards a bounded attractor in dissipative systems, it is possible to use temporal averaging of some observable $A(\mathbf{x})$ in order to sample the phase-space region visited by the dynamics and to define a stationary probability distribution $p_{\text{st}}(\mathbf{x})$:

$$\lim_{T \rightarrow \infty} \frac{1}{T} \int_0^T A(\Phi^t \mathbf{x}_0) dt = \int A(\mathbf{x}) p_{\text{st}}(\mathbf{x}) d\mathbf{x}. \quad (12)$$

The dynamical system $(\mathcal{M}, \Phi^t, p_{\text{st}})$ is ergodic if Eq. (12) holds for any observable $A(\mathbf{x})$ such that its right-hand member exists and for almost all initial conditions \mathbf{x}_0 taken with respect to the distribution p_{st} [8, 85, 86].

The system is mixing if the time correlation functions between two observables $A(\mathbf{x})$ and $B(\mathbf{x})$ decay to zero asymptotically in time, i.e., if

$$\lim_{t \rightarrow \infty} \langle A(\Phi^t \mathbf{x}) B(\mathbf{x}) \rangle = \langle A(\mathbf{x}) \rangle \langle B(\mathbf{x}) \rangle, \quad (13)$$

where $\langle \cdot \rangle$ denotes the average with respect to the stationary probability distribution $p_{\text{st}}(\mathbf{x})$. The condition (13) expresses the loss of statistical correlation between two observables separated by a long time evolution, i.e., memory loss. Mixing implies ergodicity [85, 86].

Surprisingly, these properties also hold for systems with infinitely many particles such as the ideal gases [85].

Finite-dimensional systems may have further properties such as positive and negative Lyapunov exponents for their typical trajectories and dense periodic orbits among them, as in Axiom-A systems. This class of dynamical systems has been introduced by Smale and is at the historical origin of the theory of chaotic attractors where they play a central role [8, 89, 90].

III. DYNAMICAL RANDOMNESS

A. Entropy per unit time

In order to characterize dynamical randomness, the system of interest should undergo a stroboscopic observation at regular times $t_k = k\tau$ with $k \in \mathbb{Z}$. The measuring device detects the observables with a finite resolution and records binary data for instance, as schematically shown in Fig. 1. The symbols ω_k that are recorded every time $t_k = k\tau$ correspond to some small domain in phase space. Therefore, the observation of the system with a finite resolution amounts to consider a partition $\mathcal{C} = \{C_i\}$ of its phase space \mathcal{M} into cells C_i that are supposed to be disjoint and to cover the whole phase space: $C_i \cap C_j = \emptyset$ for $i \neq j$ and $\mathcal{M} = \cup_i C_i$. These cells are of diameter ϵ . A trajectory $\mathbf{x}_t = \Phi^t \mathbf{x}_0$ of the system is recorded as a sequence of symbols ω_k corresponding to the successive cells that are visited at the times $t_k = k\tau$: $\boldsymbol{\omega} = \omega_0 \omega_1 \omega_2 \cdots \omega_{n-1}$ if $\Phi^{k\tau} \mathbf{x}_0 \in C_{\omega_k}$ for $k = 0, 1, 2, \dots, n-1$. This sequence represents the history of the system during the lapse of time $n\tau$.

The probability that a given history is realized can be expressed in terms of the stationary probability density $p_{\text{st}}(\mathbf{x})$ as

$$P(\boldsymbol{\omega}) = P(\omega_0 \omega_1 \cdots \omega_{n-1}) = \int_{C_{\boldsymbol{\omega}}} p_{\text{st}}(\mathbf{x}_0) d\mathbf{x}_0 \quad \text{with} \quad C_{\boldsymbol{\omega}} = \bigcap_{k=0}^{n-1} \Phi^{-k\tau} C_{\omega_k}. \quad (14)$$

If the system was as random as coin tossing, this probability would decay exponentially as 2^{-n} . Such an exponential decay is thus characteristic of randomness. In this respect, the entropy per unit time is introduced as the average decay rate:

$$h(\mathcal{C}) = \lim_{n \rightarrow \infty} -\frac{1}{n\tau} \sum_{\boldsymbol{\omega}} P(\boldsymbol{\omega}) \ln P(\boldsymbol{\omega}). \quad (15)$$

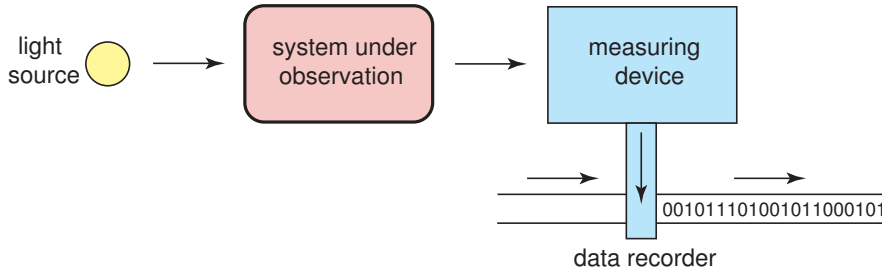


FIG. 1: Schematic representation of the observation of some system by a measuring device and the recording of the data produced by measurement.

This quantity depends on the conditions of observation given by the partition \mathcal{C} together with the sampling time τ . To get rid of these conditions, the Kolmogorov-Sinai (KS) entropy per unit time is defined as the supremum of the dynamical entropy (15) over all the possible partitions (and values of the sampling time) [8, 85, 86]:

$$h_{\text{KS}} = \text{Sup}_{\mathcal{C}} h(\mathcal{C}). \quad (16)$$

The KS entropy represents the minimum data accumulation rate required to reconstruct the trajectory of the system in phase space. In this sense, it represents the rate of production of information during data recording.

The entropy per unit time (15) is the analogue of the entropy per unit volume defined in statistical mechanics to characterize disorder in the degrees of freedom for a system at thermodynamic equilibrium. From this viewpoint, it is the temporal disorder that is characterized by the entropy per unit time (15).

Periodic or quasiperiodic signals have a vanishing entropy per unit time. Since a positive entropy means that randomness is extensive in time, a system is not necessarily devoid of randomness if it has a vanishing entropy per unit time. This is the case for sporadic systems manifesting intermittency where the probabilities (14) have subexponential decay in time: $-\ln P(\boldsymbol{\omega}) \sim n^{\nu_0} (\ln n)^{\nu_1}$ with $0 < \nu_0 < 1$ or $\nu_0 = 1$ and $\nu_1 < 0$ as $n \rightarrow \infty$ [91, 92]. Such behavior is often the feature of complex time evolution based on nested logical rules [93].

B. Deterministic dynamical systems

In deterministic dynamical systems with a bounded phase space or attractor, the KS entropy is related to the positive average Lyapunov exponents according to Pesin's formula [8]:

$$h_{\text{KS}} = \sum_{\bar{\lambda}_i > 0} \bar{\lambda}_i. \quad (17)$$

In this regard, the system is said to be chaotic if its KS entropy per unit time is positive. This quantity has been evaluated, in particular, for dilute gases in equilibrium [94, 95].

If the system is open and trajectories escape from it at the rate γ , the KS entropy is reduced to the value [8, 96, 97]:

$$h_{\text{KS}} = \sum_{\bar{\lambda}_i > 0} \bar{\lambda}_i - \gamma, \quad (18)$$

which is the case in scattering systems with trajectories trapped in the region of the scatterer, as in the three-disk billiard [31, 98]. In the two-disk billiard, there is a single trapped trajectory, which is periodic and bouncing between the two disks. In this billiard, the KS entropy is vanishing and the escape rate is thus equal to the positive Lyapunov exponent: $\gamma = \lambda_1 > 0$. This example shows that positive Lyapunov exponents are not always characterizing dynamical randomness, although the KS entropy does.

The invariant set of trajectories that are trapped in the scatterer or the attractor often form a fractal [87, 88, 98–101]. Partial dimensions $0 \leq d_i \leq 1$ may be associated with every Lyapunov exponent $\bar{\lambda}_i$ and the overall information dimension of the invariant set is given by $D_{\text{I}} = \sum_i d_i$, while the KS entropy (18) becomes $h_{\text{KS}} = \sum_{\bar{\lambda}_i > 0} d_i \bar{\lambda}_i$ [8, 102, 103]. The partial dimension corresponding to the direction of the flow takes the unit value. In chaotic systems with a three-dimensional phase space, the Lyapunov exponents are $\bar{\lambda}_1 > \bar{\lambda}_2 = 0 > \bar{\lambda}_3$ and the so-called information dimension is given by Young's formula [8]:

$$D_{\text{I}} = h_{\text{KS}} \left(\frac{1}{\bar{\lambda}_1} + \frac{1}{|\bar{\lambda}_3|} \right) + 1. \quad (19)$$

In dissipative dynamical systems with a three-dimensional phase space as for the Lorenz system [7, 8], the attractor is smooth in the unstable direction and the direction of the flow, but fractal in the stable direction. Consequently, the partial dimensions are $d_1 = h_{\text{KS}}/\bar{\lambda}_1 = 1$, $d_2 = 1$, and $0 < d_3 = h_{\text{KS}}/|\bar{\lambda}_3| < 1$, so that the information dimension is equal to $D_I = 2 + d_3$.

In open systems such as the three-disk scatterer, energy is conserved and the phase space is therefore taken as a three-dimensional energy shell. The average Lyapunov exponents are $\bar{\lambda}_1 > \bar{\lambda}_2 = 0 > \bar{\lambda}_3 = -\bar{\lambda}_1$, because the flow is symplectic. The fractal of trapped trajectories has an information dimension equal to $D_I = 2d_1 + 1$ with $d_1 = d_3 = h_{\text{KS}}/\bar{\lambda}_1 = 1 - \gamma/\bar{\lambda}_1$ and $d_2 = 1$ [31, 88, 98–100].

These properties have also been investigated for open Lorentz gases with periodic or random configurations of disks [27, 28, 31, 98, 104].

The entropy per unit time can also be defined for quantum systems, as shown by Connes, Narnhofer, and Thirring [105]. This dynamical entropy is vanishing for bounded quantum systems with a finite number of particles and can be positive for infinitely large quantum systems with a positive temperature, thus manifesting quantum chaos [106].

C. Stochastic processes

In stochastic processes such as Markovian jump processes, Brownian motion, or Langevin processes, the KS entropy per unit time is infinite because randomness is generated on arbitrarily small scales of space or time. Accordingly, stochastic processes have a higher degree of randomness than chaotic dynamical systems. In order to better characterize this degree, we need to fix the size ϵ of the cells or the sampling time τ and define an (ϵ, τ) -entropy per unit time with Eq. (15) [46, 107, 108].

For Markovian jump processes ruled by the master equation

$$\frac{dP_\omega}{dt} = \sum_{\omega' (\neq \omega)} (W_{\omega\omega'} P_{\omega'} - W_{\omega'\omega} P_\omega), \quad (20)$$

the states $\{\omega\}$ are discrete, but the lapses of time that the system is waiting in a state ω between two successive jumps are continuous random variables [109]. As a consequence, the (ϵ, τ) -entropy per unit time behaves as $h(\tau) \sim \ln(1/\tau)$ where the dependence on ϵ has disappeared because the states $\{\omega\}$ are discrete [46]. This τ -entropy takes larger and larger values as the process is observed with smaller and smaller sampling times, meaning that randomness is generated on arbitrarily small time scales in such processes.

For Brownian motion or Langevin processes described by the stochastic differential equations (5), the trajectories manifest randomness on arbitrarily small scales in the variables \mathbf{x} . This randomness comes from the Gaussian white noises, so that the ϵ -entropy per unit time scales as $h(\epsilon) \sim 1/\epsilon^2$ [46]. This behavior can be observed experimentally in Brownian motion [110]. Since the resolution scale ϵ could take smaller and smaller values without apparent saturation of this ϵ -entropy per unit time, we would conclude that the degree of randomness is higher for Brownian motion than for deterministic dynamical systems, as assumed in the stochastic theory of Wiener process. We may wonder how the scaling $h(\epsilon) \sim 1/\epsilon^2$ would be modified in the inertial regime, which can nowadays be observed [111].

The (ϵ, τ) -entropy per unit time has also been measured for turbulence [112–114]. Different scalings in ϵ and τ , as well as different types of extensivity in space or time, can manifest themselves in stochastic processes [46]. For quantum ideal gases, the product of the position-momentum or energy-time resolutions is bounded by Planck's constant, so that the (ϵ, τ) -entropy per unit time saturates at the value given by Connes, Narnhofer, and Thirring [105, 115].

Beyond the concept of temporal disorder, the study of large-deviation dynamical properties has been developed for stochastic processes in analogy with dynamical systems theory, in particular, to identify dynamical transitions in space-time stochastic processes [47–51].

D. Implications of symmetry breaking

Symmetry-breaking phenomena can manifest themselves at the level of temporal disorder characterized by the entropy per unit time. The following method can be used in order to detect such phenomena by time-series analysis. We suppose that the dynamical system of interest is symmetric under a group G of transformations:

$$\Phi^t \circ \mathbf{g} = \mathbf{g} \circ \Phi^t, \quad \forall \mathbf{g} \in G. \quad (21)$$

The partition \mathcal{C} of its phase space should be compatible with this symmetry group in the sense that the group elements map the partition onto itself, i.e., there exists a cell $C_j \in \mathcal{C}$ such that $C_j = \mathbf{g}C_i$, $\forall C_i \in \mathcal{C}$ and $\forall \mathbf{g} \in G$. In this case,

we can compare the decay rate of the probability (14) with the decay rate of the probability $P^{\mathbf{g}} = P(\boldsymbol{\omega}^{\mathbf{g}})$ of the symmetric history $\boldsymbol{\omega}^{\mathbf{g}}$. Averaging over the typical histories, we introduce the coentropy per unit time as

$$h^{\mathbf{g}}(\mathcal{C}) = \lim_{n \rightarrow \infty} -\frac{1}{n\tau} \sum_{\boldsymbol{\omega}} P(\boldsymbol{\omega}) \ln P(\boldsymbol{\omega}^{\mathbf{g}}). \quad (22)$$

The difference between this coentropy and the entropy per unit time (15) is a Kullback-Leibler divergence between the probability distribution P and $P^{\mathbf{g}}$

$$D_{\text{KL}}(P||P^{\mathbf{g}}) = h^{\mathbf{g}}(\mathcal{C}) - h(\mathcal{C}) = \lim_{n \rightarrow \infty} \frac{1}{2n\tau} \sum_{\boldsymbol{\omega}} [P(\boldsymbol{\omega}) - P(\boldsymbol{\omega}^{\mathbf{g}})] \ln \frac{P(\boldsymbol{\omega})}{P(\boldsymbol{\omega}^{\mathbf{g}})} \geq 0, \quad (23)$$

which is always non negative because $(x-y) \ln(x/y) \geq 0$ for real values of x and y [116]. It is vanishing if both probability distributions coincide, in which case the probability distribution $P(\boldsymbol{\omega})$ is symmetric under the transformation \mathbf{g} . Otherwise, the symmetry is broken by the probability distribution: $P(\boldsymbol{\omega}) \neq P(\boldsymbol{\omega}^{\mathbf{g}})$. In the presence of symmetry breaking, the coentropy would be larger than the entropy, $h^{\mathbf{g}} > h$, so that the symmetric histories $\boldsymbol{\omega}^{\mathbf{g}}$ would be less probable than the typical ones $\boldsymbol{\omega}$. This powerful method can be applied not only to symmetry-breaking phenomena in dynamical systems, but also in equilibrium statistical mechanics [117].

E. Time-reversal symmetry breaking

The previous considerations also concern time reversal. The time-reversed history $\boldsymbol{\omega}^{\text{R}} = \omega_{n-1} \cdots \omega_2 \omega_1 \omega_0$ could have a probability $P^{\text{R}} = P(\boldsymbol{\omega}^{\text{R}})$ different from the history probability (14). The coentropy per unit time

$$h^{\text{R}}(\mathcal{C}) = \lim_{n \rightarrow \infty} -\frac{1}{n\tau} \sum_{\boldsymbol{\omega}} P(\boldsymbol{\omega}) \ln P(\boldsymbol{\omega}^{\text{R}}) \quad (24)$$

would test if the time-reversed histories are equiprobable or less probable than the typical histories whether $h^{\text{R}} = h$ or $h^{\text{R}} > h$, respectively [52].

This analysis has been carried out in particular for driven Brownian motion and noise in a driven RC electric circuit [53, 54]. The fundamental result is that the difference between the coentropy (24) and the entropy per unit time (15) gives the *thermodynamic* entropy production, i.e., the power dissipated by driving the Brownian particle or the electric circuit away from equilibrium:

$$\frac{d_i S}{dt} = \lim_{\varepsilon, \tau \rightarrow 0} k_{\text{B}} [h^{\text{R}}(\varepsilon, \tau) - h(\varepsilon, \tau)] \geq 0, \quad (25)$$

where k_{B} denotes Boltzmann's constant. Therefore, thermodynamic entropy production results from time-reversal symmetry breaking in the property of dynamical randomness, alias, temporal disorder. Figure 2 shows that this irreversibility (or thermodynamic arrow of time) is experimentally observed down to the nanometric scale in the position of the driven Brownian particle and down to a few thousand electron charges in the driven electric circuit. Using methods from dynamical systems theory, this experiment has thus performed one of the most stringent tests of the second law of thermodynamics [53, 54].

The method based on Eq. (25) to evaluate irreversibility by comparing the information content of time-reversed processes has been further developed [118–121]. In particular, this method has provided a powerful approach to understand Landauer's principle [122], according to which thermodynamic entropy is produced during the erasure of information [52, 119, 123, 124].

IV. TRACE FORMULAS, CYCLES, AND DECAY RATES

If the mixing property assumes the decay of time correlation functions, we may wonder whether there exist complex decay rates that characterize the system of interest. This question can be answered by analyzing the linear operator ruling time evolution for the process of interest, which is the Liouvillian operator (7) for deterministic systems.

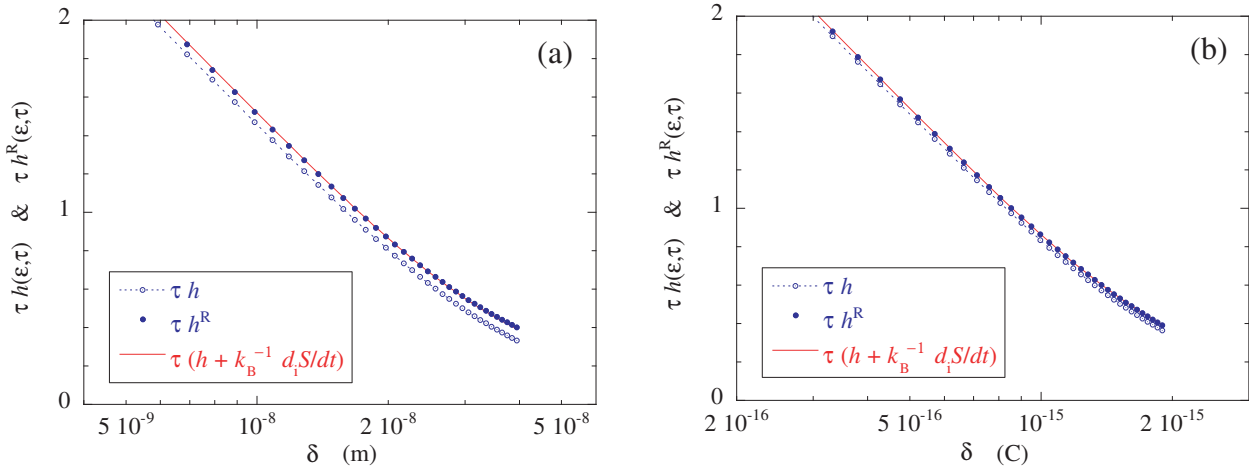


FIG. 2: (a) Brownian particle of viscous friction coefficient $\alpha = 2.93 \times 10^{-8}$ kg/s in an optical trap $V = k(z - ut)^2/2$ of stiffness $k = 9.62 \times 10^{-6}$ kg/s² moving at the speed $u = 4.24 \times 10^{-6}$ m/s in water at $T = 298$ K: (ε, τ) -entropy h and time-reversed coentropy h^R per unit time scaled by the sampling time $\tau = 1/2048$ s as a function of $\delta = \varepsilon/\sqrt{1 - \exp(-2\tau/\tau_R)}$ with the relaxation time $\tau_R = \alpha/k = 3.05 \times 10^{-3}$ s. The unit of δ is the meter (m). The entropy production is evaluated as $\frac{1}{k_B} \frac{d_i S}{dt} = \alpha u^2/(k_B T) = 128$ s⁻¹. (b) RC electric circuit with resistance $R = 9.22$ M Ω and capacitance $C = 278$ pF at the temperature $T = 298$ K driven by the current $I = 1.67 \times 10^{-13}$ A: (ε, τ) -entropy h and time-reversed coentropy h^R per unit time scaled by the sampling time $\tau = 1/2048$ s as a function of $\delta = \varepsilon/\sqrt{1 - \exp(-2\tau/\tau_R)}$ with $\tau_R = RC = 2.56 \times 10^{-3}$ s. The unit of δ is here the Coulomb (C). The entropy production is evaluated as $\frac{1}{k_B} \frac{d_i S}{dt} = RI^2/(k_B T) = 62.5$ s⁻¹. In both panels, the solid line is the result expected from Eq. (25). Reproduced with permission from D. Andrieux, P. Gaspard, S. Ciliberto, N. Garnier, S. Joubaud, and A. Petrosyan, *Journal of Statistical Mechanics: Theory and Experiment*, P01002 (2008). Copyright 2008 IOP Publishing Ltd.

A. Stochastic processes

For Markovian jump processes ruled by the master equation (20), the decay rates can be obtained as the poles of the resolvent. Its trace can be written in terms of the matrix of the transition rates $\mathbf{W} = (W_{\omega\omega'})$ as

$$\text{tr} \frac{1}{s - \mathbf{W}} = \frac{\partial}{\partial s} \ln Z(s), \quad (26)$$

where the zeta function is here the characteristic determinant of the matrix:

$$Z(s) = \det(s \mathbf{1} - \mathbf{W}). \quad (27)$$

For a system with a finite number M of states $\{\omega\}$, the zeta function is a polynomial of degree M , which admits so many complex roots $\{s_k\}$. Accordingly, the time evolution of the process can be decomposed into the exponential functions $\exp(s_k t)$. Since the total probability is conserved by the master equation (20), the leading root is equal to zero $s_0 = 0$, while the other roots should have a negative real part $\text{Re } s_k < 0$ and give the decay rates $\gamma_k = -\text{Re } s_k$ of the time correlation functions.

B. Deterministic dynamical systems

The idea of this method extends to Axiom-A dynamical systems, in which the periodic orbits – i.e., the cycles – are unstable and dense in the invariant set of trajectories, as shown by Cvitanović and Eckhardt [40, 41]. The zeta function is an infinite product over all the prime periodic orbits and its zeros give the so-called Pollicott-Ruelle resonances controlling the decay of the time correlation functions [125–127]. Such analyses have been carried out in particular for the Lorenz attractor [128], as well as for moderate turbulence [129–131]. A related method has also been developed for fluid flows [132]. In open systems, the leading Pollicott-Ruelle resonance gives the escape rate $\gamma = -s_0$, while the other resonances control finer time dependences in the oscillating decay of the time-dependent probabilities [133].

C. Noisy systems

This powerful method of analysis has also been extended to noisy systems in the weak-noise limit, which is similar but different from the semiclassical limit in quantum systems. Instead of obtaining Gutzwiller's trace formula [45], a different trace formula can be deduced that reduces to the Cvitanović-Eckhardt formula in the noiseless limit [42, 43]. The result applies to periodic or chaotic attractors subjected to noise. For noisy oscillators, the time correlation functions present damped oscillations due to phase diffusion and the correlation time of the oscillations can be calculated [43]. In other systems, the noise activates transitions or escape as in nucleation processes. Here also, the method can be developed to obtain the leading rate, which vanishes exponentially fast in the noiseless limit [44].

V. TRANSPORT

Spatially extended systems may sustain transport processes such as diffusion, viscosity, or heat conductivity. These processes are closely associated with the conservation laws of particle number, momentum, and energy. For this reason, the modes carrying out transport are slow with respect to the other degrees of freedom. These hydrodynamic modes have decay rates vanishing as their wavelength becomes infinite, in which limit the conservation laws are recovered [24].

The methods developed in dynamical systems theory to obtain the decay rates also apply to spatially extended systems and they allow us to investigate transport processes in detail. Different approaches have been followed in order to explain how exponentially decaying modes can emerge in deterministic Hamiltonian systems that are time-reversal symmetric and obey Liouville's theorem.

A. Escape-rate formalism

In scattering theory – which is fundamental to interpret experiments in atomic, molecular, particle, and mesoscopic physics – systems are open with particles coming in free flight from infinity, colliding in a bounded region, to be scattered and move away to infinity in free flight again. These systems are ruled by quantum or classical Hamiltonian dynamics. An example is provided by the three-disk scatterer, in which a point particle undergoes elastic collisions on a scatterer composed of three disks fixed in the plane [31, 88, 98–100]. Most of the trajectories of the point particle are bouncing a finite number of times on the disks between their incoming and outgoing free flights. However, there exist a fractal set of trapped trajectories bouncing forever between the disks. These trajectories are nevertheless unstable so that nearby trajectories escape from this set at a rate γ given by Eq. (18) in terms of the Lyapunov exponents and the KS entropy per unit time [8, 96, 97].

Now, the scatterer may be composed by many fixed disks forming a regular lattice of finite extension, as a slab of the hard-disk Lorentz gas with a finite horizon [27, 28]. As long as the particle remains trapped inside this large scatterer, it undergoes a random walk characterized by a diffusion coefficient \mathcal{D} , but the particle escapes to infinity as soon as it reaches the boundary of the scatterer. If the slab has a width L (much larger than the interdisk distance), the escape rate is thus given by

$$\gamma = \mathcal{D} \left(\frac{\pi}{L} \right)^2. \quad (28)$$

Combining with Eq. (18), we obtain a relationship between the diffusion coefficient and the characteristic quantities of chaos in the scatterer:

$$\mathcal{D} = \lim_{L \rightarrow \infty} \left(\frac{L}{\pi} \right)^2 (\bar{\lambda}_1 - h_{\text{KS}})_L \quad (29)$$

for a two-dimensional Lorentz gas of Lyapunov exponents $\bar{\lambda}_1 > \bar{\lambda}_2 = 0 > \bar{\lambda}_3 = -\bar{\lambda}_1$. In the three-dimensional phase space \mathcal{M}_E formed by an energy shell, the fractal set of trapped trajectories has the information dimension:

$$D_{\text{I}} = 3 - 2 \frac{\mathcal{D}}{\bar{\lambda}_1} \left(\frac{\pi}{L} \right)^2 + O(L^{-3}). \quad (30)$$

Similar considerations apply to the other transport coefficients, which are the shear and bulk viscosities and heat conductivity [29]. However, these transport properties are the features of systems with interacting particles. Here,

the escape should not be conceived as the escape of independent particles, but as the escape of the trajectories of the many-particle system out of a domain in its high-dimensional phase space. This domain should be defined by requiring that the centroid of the conserved quantity associated with the transport property of interest remains inside a given interval. These centroids are called Helfand moments and they are defined for every transport coefficient [134]. For shear viscosity, the Helfand moment is defined as

$$G^{(\eta)} = \frac{1}{\sqrt{V k_B T}} \sum_{j=1}^N x_j p_{jy} \quad (31)$$

in terms of the coordinates x_j and p_{jy} of the positions and momenta of the N particles of a fluid contained in a volume V and the temperature T [29]. Any value of the Helfand moment corresponds to a hypersurface in the phase space $V^N \otimes \mathbb{R}^{3N}$ of the N -particle system. Therefore, the condition that the Helfand moment remains inside the interval $G^{(\eta)} \in [-\chi/2, +\chi/2]$ defines a domain in the phase space, from which the trajectories will eventually escape. Now, the Helfand moment is known to undergo a random walk motion with a diffusivity precisely equal to the transport coefficient, i.e., shear viscosity η . Accordingly, the rate of escape of the so-defined phase-space domain can be evaluated as $\gamma = \eta(\pi/\chi)^2$ in analogy with Eq. (28), whereupon shear viscosity can be expressed in terms of the Lyapunov exponents and the KS entropy per unit time as [29]

$$\eta = \lim_{\chi, V, N \rightarrow \infty} \left(\frac{\chi}{\pi} \right)^2 \left(\sum_{\bar{\lambda}_i > 0} \bar{\lambda}_i - h_{\text{KS}} \right)_{\chi, V, N}. \quad (32)$$

This method has been numerically validated for diffusion as well as viscosity [28, 135].

B. Fractal diffusive modes

Periodic boundary conditions are often considered to perform molecular dynamics simulations, in particular, to calculate the transport coefficients with the Green-Kubo formulas [32]. In such simulations, transport is studied by counting some winding numbers around the multidimensional torus \mathbb{T}^{3N} , which forms the configuration space.

For the diffusion of a tracer particle, the winding numbers are associated with the motion of the particle from cell to cell in an infinite lattice. As a consequence, Bloch's theorem can be considered for the Liouvillian dynamics of the system together with the winding numbers. The full dynamics on the lattice can be decomposed into sectors with a given wavenumber \mathbf{k} belonging to the first Brillouin zone of the reciprocal lattice. All these sectors have decoupled dynamics and can be solved separately [136, 137]. Therefore, the Pollicott-Ruelle resonances $s_{\mathbf{k}}$ of each sector depend on the wavenumber \mathbf{k} . As the wavenumber vanishes, i.e., as the wavelength tends to infinity, the leading Pollicott-Ruelle resonance is expected to give the dispersion relation of diffusion: $s_{\mathbf{k}} = -\mathcal{D}\mathbf{k}^2 + O(\mathbf{k}^4)$ [31, 137, 138]. Remarkably, the associated eigenmode can be constructed for simple models such as the multibaker map, the hard-disk Lorentz gas, as well as the Yukawa-potential Lorentz gas [33]. This eigenmode $\Psi_{\mathbf{k}}(\Gamma)$ is given by a distribution of Gelfand-Schwartz type that can be represented by the cumulative function:

$$F_{\mathbf{k}}(\theta) = \int_0^\theta \Psi_{\mathbf{k}}(\Gamma_{\theta'}) d\theta' = \lim_{t \rightarrow \infty} \frac{\int_0^\theta d\theta' \exp[i\mathbf{k} \cdot (\mathbf{r}_t - \mathbf{r}_0)_{\theta'}]}{\int_0^{2\pi} d\theta' \exp[i\mathbf{k} \cdot (\mathbf{r}_t - \mathbf{r}_0)_{\theta'}]}, \quad (33)$$

where $\Gamma_\theta \in \mathcal{M}_E$ denotes a phase-space point taken at an angle $0 \leq \theta < 2\pi$ around a circle enclosing an obstacle of the Lorentz gas, for instance, and \mathbf{r}_t is the position (i.e., the vector of winding numbers) of the tracer particle in the periodic lattice [33].

Figure 3 shows the cumulative function of the diffusive modes for the different aforementioned models. The cumulative function (33) takes complex values and turns out to depict a fractal curve in the complex plane. Its Hausdorff dimension $0 \leq D_H \leq 2$ is related to the wavenumber \mathbf{k} , the diffusion coefficient \mathcal{D} , and the average positive Lyapunov exponent $\bar{\lambda}_1$ according to

$$D_H = 1 + \frac{\mathcal{D}}{\bar{\lambda}_1} \mathbf{k}^2 + O(\mathbf{k}^4), \quad (34)$$

which is reminiscent of Eq. (30) [33]. The distributions of these diffusive modes are fractal in the stable phase-space direction, but smooth along the unstable direction. Since time reversal exchanges these directions, the Liouvillian construction of the diffusive modes reveals the symmetry breaking of time reversal at the statistical level of description [31, 136, 139].

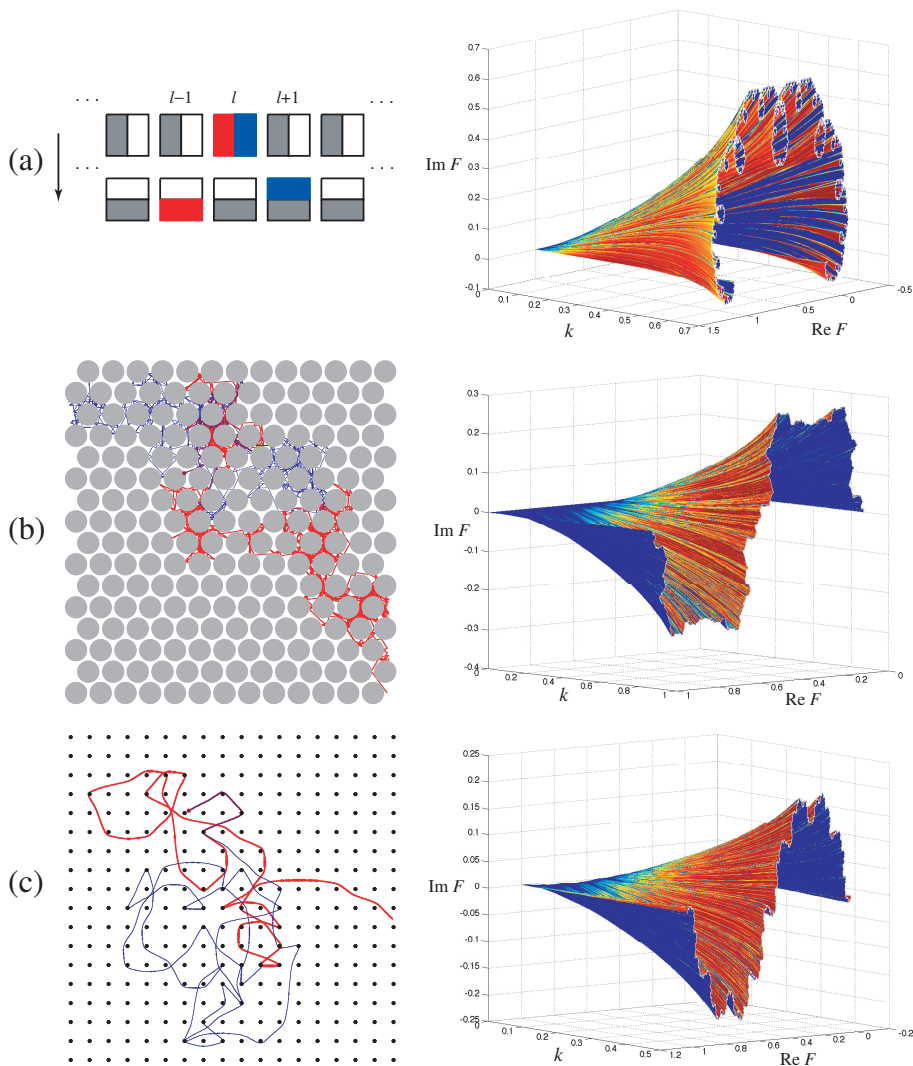


FIG. 3: The diffusive modes in (a) the multibaker map, (b) the hard-disk Lorentz gas, and (c) the Yukawa-potential Lorentz gas. The left-hand column illustrates the mechanism of diffusion of particles in these systems. In the right-hand column, the cumulative function (33) is depicted in the complex plane ($\text{Re } F, \text{Im } F$) versus the wavenumber k , for each system. For the two-dimensional Lorentz gases, the wavenumber k is taken in the horizontal direction. If the wavenumber vanishes $k = 0$, the cumulative function reduces to the straight line $\text{Im } F = 0$ between the points $\text{Re } F = 0$ and $\text{Re } F = 1$, which represents the microcanonical equilibrium state.

C. Entropy production

In the limit where the wavenumber vanishes $\mathbf{k} \rightarrow 0$, any diffusive mode tends to the microcanonical equilibrium state, but its derivative with respect to the wavenumber gives the distribution associated with a nonequilibrium steady state [136, 137]. Indeed, a diffusive mode decaying as $\exp(-\mathcal{D}k^2t)$ behaves in space as $\sin(kx)$ at the macroscopic level of description. Taking its derivative with respect to the wavenumber k and the limit $k \rightarrow 0$ gives the linear profile of concentration x expected for a nonequilibrium steady state. Fick's law can be recovered by averaging the flux of particles over the so-obtained distribution [136, 137]. As it should, the diffusion coefficient is given by the Green-Kubo formula, demonstrating the consistency of the phase-space construction for the diffusive modes [31]. We notice that the nonequilibrium steady states also have distributions breaking the time-reversal symmetry, because they are smooth in the unstable phase-space direction, but fractal-like in the stable one [33, 136].

Furthermore, the fractal character of the diffusive modes justifies the use of coarse graining in order to define a time-dependent thermodynamic entropy in phase space. Since the dynamics of the multibaker map and Lorentz gases is mixing, the time correlation functions are decaying to zero and the time-dependent probabilities to their

equilibrium values. Accordingly, the coarse-grained entropy is converging to its equilibrium value asymptotically in time. The remarkable result is that the corresponding rate of thermodynamic entropy production takes the value given by macroscopic theory as the consequence of the fractal character of the diffusive modes, which establishes the second law of thermodynamics directly from Liouvillian dynamics and down to very small coarse-graining scales in phase space [140].

Similar or related conclusions have been reached in different approaches [141–143].

D. Time-reversal symmetry relation for current fluctuations

In the Lorentz gases or the multibaker map, a nonequilibrium steady state can be maintained if the diffusive medium is located between two infinite particle reservoirs at different concentrations [136, 137]. Fick’s law is satisfied by the continuous average flux of particles from the high- to the low-concentration reservoir. Most trajectories of this state belong to the phase-space set that is complementary to the set of trapped trajectories together with its stable and unstable manifolds. The number ΔN_t of particles flowing from the left- to the right-hand reservoir during the time interval $[0, t]$ obeys the relation:

$$\frac{P(\Delta N_t)}{P(-\Delta N_t)} \simeq_{t \rightarrow \infty} \exp(A \Delta N_t) \quad (35)$$

in terms of the affinity $A = \ln(n_L/n_R)$, where n_L and n_R are the reservoir concentrations [57–59]. This general result is a consequence of the time-reversal symmetry of the microscopic dynamics and is already established for effusion through a small hole in a planar wall between the reservoirs [63]. Since the particle concentrations are different in both reservoirs, the probability weight of the trajectories going from the left- to the right-hand reservoir is different from the one of the reversed trajectories, which implies Eq. (35). We notice that the scale of coarse graining is here taken at the macroscale in partitioning the system between two domains, each one including a reservoir. This scale is enough to obtain the overall rate of entropy production $\frac{1}{k_B} \frac{d_i S}{dt} = A \langle J \rangle$ in terms of the affinity A and the average particle flux $\langle J \rangle = \lim_{t \rightarrow \infty} \langle \Delta N_t \rangle / t$. Stronger conditions on the dynamics allow us to decrease the scale of coarse graining at which the second law holds.

Fluctuation relations such as Eq. (35) have been proved for different quantities in broad classes of dynamical and stochastic systems [34–36, 55–63].

E. Fourier’s law in many-particle billiards

Recently, heat conduction has been studied in many-particle billiards where particles are bouncing inside traps forming a lattice [37–39]. The particles cannot move to neighboring traps, but they can have binary collisions with the neighboring particles, thus, exchanging kinetic energy. Hence, kinetic energy can be transported in the lattice without mass transport. If the particles are hard disks and the traps are chaotic billiards, the many-particle dynamics is chaotic. In the limit where the binary collisions are very rare with respect to the collisions each particle performs in its own trap, the energy exchange process can be described by a kinetic equation, which is deduced from the pseudo-Liouville equation. At the macroscale, this kinetic equation leads to Fourier’s heat equation with an analytic expression for the transport coefficient of heat conductivity. Accordingly, this class of dynamical systems is very promising to establish a rigorous proof of Fourier’s law [144].

VI. CONCLUSIONS AND PERSPECTIVES

In this paper, an overview is given of advances at the frontier between dynamical systems theory and nonequilibrium statistical mechanics. Dynamical systems theory has introduced and developed the use of large-deviation dynamical properties, allowing us to study different aspects of dynamical randomness, i.e., temporal disorder.

In finite-dimensional deterministic systems, the origin of dynamical randomness holds in the property of sensitivity to initial conditions characterized by positive Lyapunov exponents. Beyond Lyapunov’s horizon of predictability, the dynamics should be described in terms of probability. In the probabilistic approach, the time evolution is ruled by the generalized Liouvillian equation [25], which can be solved to get the stationary probability distribution and the eigenmodes of relaxation associated with the decay rates, called Pollicott-Ruelle resonances [125–127]. The eigenmodes of the Liouvillian dynamics can be constructed in phase space for spatially extended systems sustaining deterministic diffusion [33]. In this way as well as with the escape-rate formalism [27–31], relationships can be established between

chaotic and transport properties. In such frameworks, the thermodynamic entropy production can be obtained by coarse graining the phase space down to arbitrarily small scales [140], which provides a fundamental understanding of irreversibility in the class of chaotic dynamical systems.

Dynamical randomness can also be characterized in stochastic processes thanks to the (ϵ, τ) -entropy per unit time, which is the average decay rate for the probabilities of the histories of the system observed with a sampling time τ and a resolution ϵ [46]. If the time evolution has some possible symmetries that could be broken by the stationary probability distribution, a coentropy can be associated with the probabilities of the symmetry-transformed histories. The difference between the coentropy and the entropy per unit time is a Kullback-Leibler divergence, which detects symmetry breaking and measures its amount in the time series of the process under study.

With respect to microreversibility, the difference between the time-reversed coentropy and the entropy per unit time turns out to be equal to the *thermodynamic entropy production* in stochastic processes modeling nonequilibrium systems [52]. This theoretical prediction has been tested experimentally providing evidence for irreversibility down to very small sizes of fluctuations in driven Brownian motion and a *RC* electric circuit [53, 54]. In this way, thermodynamic entropy production can be related to time asymmetry in temporal disorder for systems driven away from equilibrium. On larger scales of coarse graining, the fluctuation relations have also been deduced as a consequence of microreversibility, yet characterizing the breaking of time-reversal symmetry under nonequilibrium conditions [34–36, 55–63]. All these results constitute a major breakthrough during the last 25 years.

To conclude, the methods of dynamical systems theory have opened new promising avenues in the study of nonequilibrium processes. Cross-fertilization is generating broad perspectives at this frontier with so many open problems in the understanding of dynamical randomness. The development of new concepts and powerful mathematical methods based on large-deviation theory, also called the thermodynamic formalism [90, 102, 103, 145, 146], allows us to explain the large variety of phenomena we observe in terms of the fundamental equations of nature, even if these phenomena seem to contradict properties that were presupposed for these equations, as the history of chaos theory shows. Even today, it is surprising and fascinating to realize that ordinary or partial differential equations may admit aperiodic solutions that can be described as random processes. Beyond the systems covered in this overview, many other phenomena are concerned: hydrodynamic, plasma, and wave turbulences, spatiotemporal chaos in reaction-diffusion systems, or structure formation in self-gravitating systems. Do we understand all the implications of the known equations of nature?

Acknowledgments

This research is financially supported by the Université Libre de Bruxelles and the Belgian Science Policy Office under the Interuniversity Attraction Pole project P7/18 “DYGEST”.

-
- [1] A. L. Cauchy, *Ordinary differential equations: unpublished course* (Johnson Reprint Corporation, New York, 1981).
 - [2] V. I. Arnold, *Ordinary differential equations* (MIT Press, Cambridge MA, 1973).
 - [3] S. von Kowalevsky, *Journal für die reine und angewandte Mathematik* **80**, 1 (1875).
 - [4] R. Courant and D. Hilbert, *Methods of Mathematical Physics*, vol. 2 (Interscience Publishers, New York, 1962).
 - [5] J. C. Maxwell, *Essay on science and free will*, in: L. Campbell and W. Garnett, *The Life of James Clerk Maxwell* (Cambridge University Press, Cambridge UK, 2010) pp. 434-444.
 - [6] H. Poincaré, *Calcul des probabilités*, 2nd edition (Paris, Gauthier-Villars, 1912) pp. 4-10.
 - [7] E. N. Lorenz, *J. Atmos. Sci.* **20**, 130 (1963).
 - [8] J.-P. Eckmann and D. Ruelle, *Rev. Mod. Phys.* **57**, 617 (1985).
 - [9] D. Ruelle and F. Takens, *Commun. Math. Phys.* **20**, 167 (1971).
 - [10] A. Brandstätter, J. Swift, H. L. Swinney, A. Wolf, J. D. Farmer, E. Jen, and P. J. Crutchfield, *Phys. Rev. Lett.* **51**, 1442 (1983).
 - [11] N. S. Krylov, *Works on the Foundations of Statistical Physics* (Princeton University Press, Princeton, 1979).
 - [12] H. A. Posch and W. G. Hoover, *Phys. Rev. A* **38**, 473 (1988).
 - [13] H. A. Posch and W. G. Hoover, *Phys. Rev. A* **39**, 2175 (1989).
 - [14] D. J. Evans and G. P. Morris, *Statistical Mechanics of Nonequilibrium Liquids* (Academic Press, London, 1990).
 - [15] J. L. Hudson and J. C. Mankin, *J. Chem. Phys.* **74**, 6171 (1981).
 - [16] J.-C. Roux, R. H. Simoyi, and H. L. Swinney, *Physica D* **8**, 257 (1983).
 - [17] S. K. Scott, *Chemical Chaos* (Clarendon Press, Oxford, 1991).
 - [18] H. Haken, *Phys. Lett. A* **53**, 77 (1975).
 - [19] R. G. Harrison and D. J. Biswas, *Nature* **321**, 394 (1986).
 - [20] R. M. May, *Nature* **261**, 459 (1976).

- [21] J. Wisdom, S. L. Peale, and F. Mignard, *Icarus* **58**, 137 (1984).
- [22] J. Laskar, *Nature* **338**, 237 (1989).
- [23] J. R. Buchler, J. M. Perdang, and E. A. Spiegel, Editors, *Chaos in Astrophysics* (Reidel Publishing Co., Dordrecht, 1985).
- [24] R. Balescu, *Equilibrium and Nonequilibrium Statistical Mechanics* (Wiley, New York, 1975).
- [25] G. Nicolis, *Introduction to Nonlinear Science* (Cambridge University Press, Cambridge UK, 1995).
- [26] T. Tél, P. Gaspard, and G. Nicolis, *Chaos* **8**, 309 (1998).
- [27] P. Gaspard and G. Nicolis, *Phys. Rev. Lett.* **65**, 1693 (1990).
- [28] P. Gaspard and F. Baras, *Phys. Rev. E* **51**, 5332 (1995).
- [29] J. R. Dorfman and P. Gaspard, *Phys. Rev. E* **51**, 28 (1995).
- [30] P. Gaspard and J. R. Dorfman, *Phys. Rev. E* **52**, 3525 (1995).
- [31] P. Gaspard, *Chaos, Scattering and Statistical Mechanics* (Cambridge University Press, Cambridge UK, 1998).
- [32] J. R. Dorfman, *An Introduction to Chaos in Nonequilibrium Statistical Mechanics* (Cambridge University Press, Cambridge UK, 1999).
- [33] P. Gaspard, I. Claus, T. Gilbert, and J. R. Dorfman, *Phys. Rev. Lett.* **86**, 1506 (2001).
- [34] D. J. Evans, E. G. D. Cohen, and G. P. Morriss, *Phys. Rev. Lett.* **71**, 2401 (1993).
- [35] G. Gallavotti and E. G. D. Cohen, *Phys. Rev. Lett.* **74**, 2694 (1995).
- [36] G. Gallavotti, *Phys. Rev. Lett.* **77**, 4334 (1996).
- [37] P. Gaspard and T. Gilbert, *Phys. Rev. Lett.* **101**, 020601 (2008).
- [38] P. Gaspard and T. Gilbert, *New J. Phys.* **10**, 103004 (2008).
- [39] P. Gaspard and T. Gilbert, *Chaos* **22**, 026117 (2012).
- [40] P. Cvitanović and B. Eckhardt, *J. Phys. A* **24**, L237 (1991).
- [41] P. Cvitanović, R. Artuso, R. Mainieri, G. Tanner, and G. Vattay, *Chaos: Classical and Quantum*, <http://chaosbook.org/>
- [42] P. Cvitanović, N. Sondergaard, G. Palla, G. Vattay, and C. Dettmann, *Phys. Rev. E* **60**, 3936 (1999).
- [43] P. Gaspard, *J. Stat. Phys.* **106**, 57 (2002).
- [44] J. Demaeyer and P. Gaspard, *J. Stat. Mech.* P10026 (2013).
- [45] M. C. Gutzwiller, *Chaos in Classical and Quantum Mechanics* (Springer, New York, 1990).
- [46] P. Gaspard and X.-J. Wang, *Phys. Rep.* **235**, 291 (1993).
- [47] C. Appert, H. van Beijeren, M. H. Ernst, and J. R. Dorfman, *Phys. Rev. E* **54**, R1013 (1996).
- [48] C. Appert, H. van Beijeren, M. H. Ernst, and J. R. Dorfman, *J. Stat. Phys.* **87**, 1253 (1997).
- [49] V. Lecomte, C. Appert-Rolland, and F. van Wijland, *Phys. Rev. Lett.* **95**, 010601 (2005).
- [50] M. Merolle, J. P. Garrahan, and D. Chandler, *Proc. Natl. Acad. Sci. U.S.A.* **102**, 10837 (2005).
- [51] J. P. Garrahan, R. L. Jack, V. Lecomte, E. Pitard, K. van Duijvendijk, and F. van Wijland, *Phys. Rev. Lett.* **98**, 195702 (2007).
- [52] P. Gaspard, *J. Stat. Phys.* **117**, 599 (2004).
- [53] D. Andrieux, P. Gaspard, S. Ciliberto, N. Garnier, S. Joubaud, and A. Petrosyan, *Phys. Rev. Lett.* **98**, 150601 (2007).
- [54] D. Andrieux, P. Gaspard, S. Ciliberto, N. Garnier, S. Joubaud, and A. Petrosyan, *J. Stat. Mech.* P01002 (2008).
- [55] J. Kurchan, *J. Phys. A: Math. Gen.* **31**, 3719 (1998).
- [56] G. E. Crooks, *Phys. Rev. E* **60**, 2721 (1999).
- [57] D. Andrieux and P. Gaspard, *J. Chem. Phys.* **121**, 6167 (2004).
- [58] D. Andrieux and P. Gaspard, *J. Stat. Mech.* P01011 (2006).
- [59] B. Derrida, *J. Stat. Mech.* P07023 (2007).
- [60] M. Esposito, U. Harbola, and S. Mukamel, *Rev. Mod. Phys.* **81**, 1665 (2009).
- [61] M. Campisi, P. Hänggi, and P. Talkner, *Rev. Mod. Phys.* **83**, 771 (2011).
- [62] U. Seifert, *Rep. Prog. Phys.* **75**, 126001 (2012).
- [63] P. Gaspard, *New J. Phys.* **15**, 115014 (2013).
- [64] L. Pauling and E. B. Wilson Jr., *Introduction to Quantum Mechanics With Applications to Chemistry* (McGraw-Hill, New York, 1935).
- [65] E. M. Lifshitz and L. P. Pitaevskii, *Statistical Physics, Part 2*, Volume 9 of the Course of Theoretical Physics by L. D. Landau and E. M. Lifshitz (Pergamon Press, Oxford, 1980).
- [66] J.-P. Eckmann, S. Oliffson Kamphorst, D. Ruelle, and S. Ciliberto, *Phys. Rev. A* **34**, 4971 (1986).
- [67] M. Yamada and K. Ohkitani, *J. Phys. Soc. Jpn.* **56**, 4210 (1987).
- [68] Ch. Dellago, H. A. Posch, and W. G. Hoover, *Phys. Rev. E* **53**, 1485 (1996).
- [69] H. van Beijeren and J. R. Dorfman, *Phys. Rev. Lett.* **74**, 4412 (1995).
- [70] H. van Beijeren, A. Latz, and J. R. Dorfman, *Phys. Rev. E* **57**, 4077 (1998).
- [71] R. van Zon, H. van Beijeren, and Ch. Dellago, *Phys. Rev. Lett.* **80**, 2035 (1998).
- [72] P. Gaspard and H. van Beijeren, *J. Stat. Phys.* **109**, 671 (2002).
- [73] A. S. de Wijn and H. van Beijeren, *Phys. Rev. E* **70**, 036209 (2004).
- [74] A. S. de Wijn, *Phys. Rev. E* **72**, 026216 (2005).
- [75] H. V. Kruis, D. Panja, and H. van Beijeren, *J. Stat. Phys.* **124**, 823 (2006).
- [76] A. S. de Wijn, B. Hess, and B. V. Fine, *Phys. Rev. Lett.* **109**, 034101 (2012).
- [77] C. L. Wolfe and R. M. Samelson, *Tellus A* **59**, 355 (2007).
- [78] F. Ginelli, P. Poggi, A. Turchi, H. Chaté, R. Livi, and A. Politi, *Phys. Rev. Lett.* **99**, 130601 (2007).
- [79] G. P. Morriss, *Phys. Rev. E* **85**, 056219 (2012).
- [80] F. Ginelli, H. Chaté, R. Livi, and A. Politi, *J. Phys. A: Math. Theor.* **46**, 254005 (2013).

- [81] S. McNamara and M. Mareschal, Phys. Rev. E **64**, 051103 (2001).
- [82] A. S. de Wijn and H. van Beijeren, Phys. Rev. E **70**, 016207 (2004).
- [83] J.-P. Eckmann, C. Forster, H. A. Posch, and E. Zabey, J. Stat. Phys. **118**, 813 (2005).
- [84] D. J. Robinson and G. P. Morriss, J. Stat. Phys. **131**, 1 (2008).
- [85] I. P. Cornfeld, S. V. Fomin, and Ya. G. Sinai, *Ergodic Theory* (Springer, New York, 1982).
- [86] G. Falasco, G. Saggiorato, and A. Vulpiani, Physica A **418**, 94 (2015).
- [87] E. Ott, *Chaos in dynamical systems* (Cambridge University Press, Cambridge UK, 1993).
- [88] T. Tél and M. Gruiz, *Chaotic Dynamics* (Cambridge University Press, Cambridge UK, 2006).
- [89] S. Smale, Bull. Am. Math. Soc. **73**, 747 (1967).
- [90] D. Ruelle, *Thermodynamic Formalism* (Addison-Wesley, Reading MA, 1978).
- [91] P. Gaspard and X.-J. Wang, Proc. Natl. Acad. Sci. USA **85**, 4591 (1988).
- [92] R. Venegeroles, J. Stat. Phys. **154**, 988 (2014).
- [93] G. Nicolis and C. Nicolis, *Foundations of Complex Systems* (World Scientific, New Jersey, 2007).
- [94] H. van Beijeren, J. R. Dorfman, H. A. Posch, and Ch. Dellago, Phys. Rev. E **56**, 5272 (1997).
- [95] A. S. de Wijn, Phys. Rev. E **71**, 046211 (2005).
- [96] H. Kantz and P. Grassberger, Physica D **17**, 75 (1985).
- [97] N. Chernov and R. Markarian, Bol. Soc. Brasil. Mat. **28**, 271, 315 (1997).
- [98] P. Gaspard and S. A. Rice, J. Chem. Phys. **90**, 2225, 2242, 2255 (1989).
- [99] Y.-C. Lai and T. Tél, *Transient Chaos* (Springer, New York, 2011).
- [100] J. M. Seoane and M. A. F. Sanjuán, Rep. Prog. Phys. **76**, 016001 (2013).
- [101] E. G. Altmann, J. S. E. Portela, and T. Tél, Rev. Mod. Phys. **85**, 869 (2013).
- [102] T. C. Halsey, M. H. Jensen, L. P. Kadanoff, I. Procaccia, and B. I. Shraiman, Phys. Rev. A **33**, 1141 (1986).
- [103] G. Paladin and A. Vulpiani, Phys. Rep. **156**, 147 (1987).
- [104] H. van Beijeren, A. Latz, and J. R. Dorfman, Phys. Rev. E **63**, 016312 (2000).
- [105] A. Connes, H. Narnhofer, and W. Thirring, Commun. Math. Phys. **112**, 691 (1987).
- [106] F. Benatti, T. Hudetz, and A. Knauf, Commun. Math. Phys. **198**, 607 (1998).
- [107] M. Abel, L. Biferale, M. Cencini, M. Falcioni, D. Vergni, and A. Vulpiani, Phys. Rev. Lett. **84**, 6002 (2000).
- [108] G. Boffetta, M. Cencini, M. Falcioni, and A. Vulpiani, Phys. Rep. **356**, 367 (2002).
- [109] C. W. Gardiner, *Handbook of Stochastic Methods*, 3rd edition (Springer, Berlin, 2004).
- [110] P. Gaspard, M. E. Briggs, M. K. Francis, J. V. Sengers, R. W. Gammon, J. R. Dorfman, and R. V. Calabrese, Nature **394**, 865 (1998).
- [111] T. Li and M. G. Raizen, Ann. Phys. (Berlin) **525**, 281 (2013).
- [112] X.-J. Wang and P. Gaspard, Phys. Rev. A **46**, R3000 (1992).
- [113] M. Abel, L. Biferale, M. Cencini, M. Falcioni, D. Vergni, and A. Vulpiani, Physica D **147**, 12 (2000).
- [114] F. G. Schmitt, Phys. Lett. A **342**, 448 (2005).
- [115] P. Gaspard, J. Math. Phys. **55**, 075208 (2014).
- [116] T. M. Cover and J. A. Thomas, *Elements of Information Theory*, 2nd edition (Wiley, Hoboken, 2006).
- [117] D. Lacoste and P. Gaspard, Phys. Rev. Lett. **113**, 240602 (2014).
- [118] A. Porporato, J. R. Rigby, and E. Daly, Phys. Rev. Lett. **98**, 094101 (2007).
- [119] R. Kawai, J. M. R. Parrondo, and C. Van den Broeck, Phys. Rev. Lett., **98**, 080602 (2007).
- [120] E. Roldan and J. M. R. Parrondo, Phys. Rev. Lett. **105**, 150607 (2010).
- [121] E. Roldan and J. M. R. Parrondo, Phys. Rev. E **85**, 031129 (2012).
- [122] R. Landauer, IBM J. Res. Dev. **5**, 183 (1961).
- [123] D. Andrieux and P. Gaspard, EPL **81**, 28004 (2008).
- [124] A. Bérut, A. Arakelyan, A. Petrosyan, S. Ciliberto, R. Dillenschneider, and E. Lutz, Nature **483**, 187 (2012).
- [125] M. Pollicott, Invent. Math. **81**, 413 (1985).
- [126] D. Ruelle, Phys. Rev. Lett. **56**, 405 (1986).
- [127] D. Ruelle, J. Stat. Phys. **44**, 281 (1986).
- [128] B. Eckhardt and G. Ott, Z. Phys. B **93**, 259 (1994).
- [129] Y. Lan and P. Cvitanović, Phys. Rev. E **78**, 026208 (2008).
- [130] P. Cvitanović and J. F. Gibson, Phys. Scr. T **142**, 014007 (2010).
- [131] T. Kreilos and B. Eckhardt, Chaos **22**, 047505 (2012).
- [132] I. Mezić, Annu. Rev. Fluid Mech. **45**, 357 (2013).
- [133] P. Gaspard and D. Alonso Ramirez, Phys. Rev. A **45**, 8383 (1992).
- [134] E. Helfand, Phys. Rev. **119**, 1 (1960).
- [135] S. Viscardy and P. Gaspard, Phys. Rev. E **68**, 041205 (2003).
- [136] S. Tasaki and P. Gaspard, J. Stat. Phys. **81**, 935 (1995).
- [137] P. Gaspard, Phys. Rev. E **53**, 4379 (1996).
- [138] R. Venegeroles, Phys. Rev. Lett. **99**, 014101 (2007).
- [139] D. J. Driebe, *Fully Chaotic Maps and Broken Time Symmetry* (Kluwer Acad. Publ., Dordrecht, 1999).
- [140] J. R. Dorfman, P. Gaspard, and T. Gilbert, Phys. Rev. E **66**, 026110 (2002).
- [141] W. Breyman, T. Tél, and J. Vollmer, Phys. Rev. Lett. **77**, 2945 (1996).
- [142] J. Vollmer, Phys. Rep. **372**, 131 (2002).
- [143] R. Klages, *Microscopic Chaos, Fractals and Transport in Nonequilibrium Statistical Mechanics* (World Scientific, New

Jersey, 2007).

[144] A. Grigo, K. Khanin, and D. Szász, *Nonlinearity* **25**, 2349 (2012).

[145] H. Touchette, *Phys. Rep.* **478**, 1 (2009).

[146] J. Kurchan, *Six out of equilibrium lectures*, in: T. Dauxois, S. Ruffo, and L. F. Cugliandolo, Editors, *Long-Range Interacting Systems*, Lecture Notes of the Les Houches Summer School: vol. 90, August 2008 (Oxford University Press, Oxford, 2010).